Hindawi
Advances in Materials Science and Engineering
Volume 2017, Article ID 3720403, 11 pages
https://doi.org/10.1155/2017/3720403

Research Article

Shot Peening Effect on Fatigue Crack Repaired Weldments

J. Efrain Rodriguez-Sanchez, Alejandro Rodriguez-Castellanos, and Faustino Perez-Guerrero

Instituto Mexicano del Petróleo, Eje Central Lázaro Cárdenas Norte 152, 07730 Ciudad de México, Mexico

Correspondence should be addressed to J. Efrain Rodriguez-Sanchez; ersanche@imp.mx

Received 1 March 2017; Accepted 10 April 2017; Published 30 April 2017

Academic Editor: Paolo Ferro

Fracture mechanics calculations are required to validate the safety level defined in design codes to prevent a fatigue failure. The periodic inspection-assessment cycle can lead to the implementation of a fatigue crack repair by crack removal. To improve the fatigue performance of the crack repair, residual compressive stresses induced by peening can be considered. This paper is in relation to the peening effect estimation on stress intensity factors in fatigue crack repaired weldments, since the stress intensity factor is a key parameter in fracture mechanics calculations. A set of T-butt specimens were experimentally fatigue tested and crack propagation data was gathered for the calculation of stress intensity factors. The experiments were designed to estimate the residual compressive stress depth layer and its effect on crack propagation inhibition. Experimental estimation of the peening effect on stress intensity factors in fatigue crack repaired weldments was validated by comparison against an analytical weight function solution. Experimental stress intensity factors determined from a set of fatigue tested T-butt specimens allowed estimating preliminarily that peening has a limited effect on fatigue crack propagation inhibition for edge repaired T-butt weldments subjected to bending loading.

1. Introduction

Inspection of components subjected to fatigue loading can reveal fatigue cracks presence; thus, depending on the particular component, the option of component replacement or repair in situ is an issue. In the offshore industry, repair in situ is the most feasible option, since offshore structures have to operate continuously.

Alternative to joint clamping, a fatigue crack repair procedure based on the removal of cracked material by grinding has been proposed for offshore structures [1–3]. The repair profile has a predesigned geometry to reinstate a fatigue life that can be even larger than the as welded fatigue life.

Research on improvements to fatigue crack repair for offshore structures incorporated metal filling of the ground notch by dry or wet welding to improve the fatigue performance of the repaired weldment surface [4].

This paper describes the addition of compressive residual stresses by shot peening to the ground notch surface to improve the fatigue performance of the repaired weldment. It is expected that compressive stresses improve the fatigue crack performance, since cracks grow due to the opening effect induced by tensile stresses. This research is focused on the estimation of the peening effect on stress intensity factors, since K is a key input in fracture mechanics calculations for fatigue life predictions.

Analytical estimation of K in weldments considering residual stresses is a complex task, since a distribution of residual stresses through the plate thickness during crack growth is required. For the case of a shot peened weldment, residual stresses are the result of adding residual stresses by welding plus compressive residual stresses by shot peening.

The International Institute of Welding [5] recommends fatigue tests for the verification of a procedure such as peening in the endurance range of interest. Recommended upper-bound welding residual stress profiles for use in analyses are given in Structural Integrity Assessment Procedures for European Industry [6–8].

Despite the uncertainty in estimating a weldment residual stress distribution, it is possible to estimate K values for a given crack location and geometry. Experimental measurements of residual stresses by neutron diffraction and X-ray

diffraction [9] can be done. The experimental residual stress distribution is implemented in an analytical method and K can be determined.

The most common analytical approaches to calculate K values are the weight function method and the finite element method. The weight function method has been used in many cases with welding residual stress distributions such as those proposed by Structural Integrity Assessment Procedures for European Industry and stress intensity factors associated with welding residual stresses (K_{res}) are determined [10]. There are more K_{res} calculations published [9–11] than peening residual stress intensity factors calculations [12, 13], where the concept of cohesive zone model is used with the finite element method to estimate compressive stress relaxation in shot peened specimens.

2. Peening

Peening is the process of impacting a metal surface causing plastic deformation in the surface. The impact objects can be hard small particles, a bunch of needles, a simple hammer, or a laser beam and the process would be known as shot peening, needle peening, hammer peening, or laser peening, respectively. The mechanisms of fatigue improvement using peening are cold work and residual compressive stress.

Cold work is used to improve the strength of metals by increasing the surface hardness; however, the brittleness is also increased and consequently there is a limit to which cold working may be carried out without danger of fracture. Fatigue improvement by peening is mainly due to the residual compressive stress rather than due to the cold work hardening process.

Residual compressive stress is probably the most important benefit of peening in terms of fatigue improvement. The residual stress is produced, since the surface layer of material is deformed beyond its yield point by peening; however, it cannot deform freely as the material underneath is not affected by the peening and therefore has not been plastically deformed. So, a residual stress is kept in the surface material due to the constraint imposed by the deeper layers. A graphical representation of this effect can be represented in a two-layer system [14] as shown in Figure 1.

Random high tensile loads, such as those that many components experience in service, reduce the beneficial effects of peening, since plastic deformation is caused at points of high stress concentration when the loading is applied.

Residual compressive stresses reduce the resultant range of fatigue stress and crack growth, since the applied tensile stress decreases when it is combined with the residual compressive stress. Thus, residual compressive stress does not change the applied stress range but increases R ratio (minimum stress/maximum stress), since tensile maximum stress is reduced. However, there are still difficulties in making quantitative predictions of the effect on fatigue life as a result of a particular peening process. Fracture mechanics procedures have not been easily applied for peened components; moreover, peening has a greater effect on the crack initiation phase, where fracture mechanics cannot be applied.

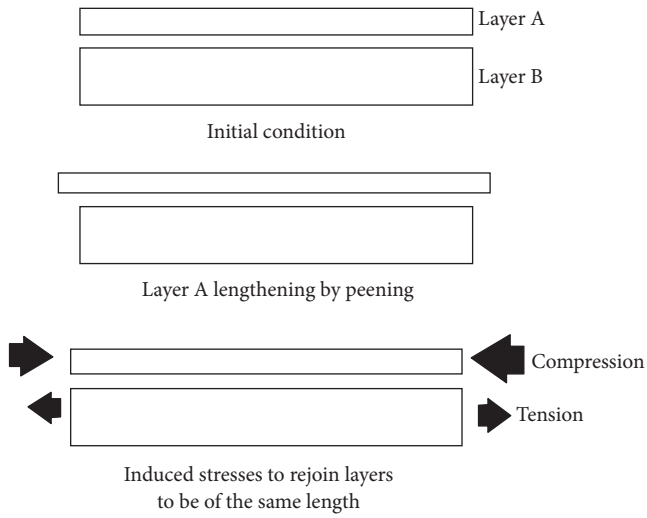

Figure 1: Creation of residual stress in a two-bar system [14].

Dissipation effect of residual compressive stress in high yield stress materials is lower, since they can sustain higher tensile loads before deforming plastically [4]. A peened surface is not smooth; thus, it may cause crack starting points. Once a crack starts to propagate across the residually compressed layers, the magnitudes of the residual stresses are needed to make predictions of crack growth, but there is not a generally reliable and practical method to obtain residual stress information.

If the shot peened component under consideration is achieving a reversed bending endurance limit close to 0.5 of the tensile strength in steels or 0.25 in other alloys, further improvement by peening is unlikely. The maximum residual compressive stress induced by shot peening is approximately 60% of the ultimate tensile strength in compression [14].

Behaviour of cracks growing from a peened surface in fatigue is that minute cracks already exist in the surface but their initial growth rate is considerably slower than that of cracks which are eventually initiated in an as welded (unpeened) surface. The crack eventually starts to grow again probably due to the residual stress relaxation by the imposed alternating stress [14].

The magnitude and depth of the residual stress field are the major factors controlling the fatigue effect of peening and these depend on the intensity of peening. For the case of shot peening, the size of the pellets determines the depth of the residual stress field [15] as can be seen in Figure 2.

Intensity will vary greatly with circumstances; one technique used in a wide variety of circumstances is to peen a flat strip of metal on one side while it is clamped to the component and then measure how much it curves when it is released. This is the Almen strip method. The strips have to be of certain dimensions and have to be made from metal with specified properties. Peening intensity is linked to this curvature, which is easily measured, as an arc-height. Large curvatures and therefore large arc-height values go with higher intensities. Almen strips are seen as a very good way of monitoring consistency of a peening process but

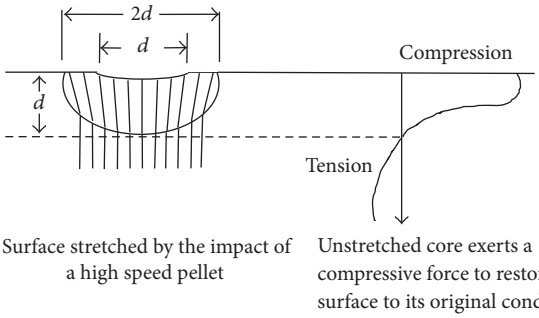

Figure 2: Depth of the residual stress field produced by shot peening [15].

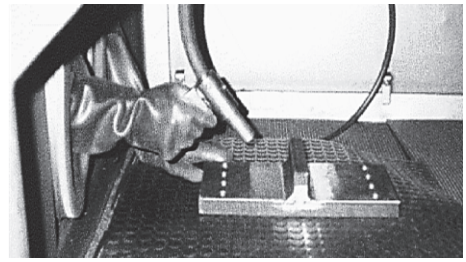

Figure 3: T-butt welded specimen during shot peening process (blast suspended).

not a fundamental way of comparing peening processes with different parameters; hence, the same curvature can be obtained by a combination of different magnitudes of the following parameters: time of exposure, blast pressure, and shot size.

Hertzian pressure theory allows estimating the stress magnitude and distribution due to the contact of two surfaces; thus, this theory can be implemented to estimate stress magnitude and distribution in a plate underneath a shot impact. However, due to the nature of the shot peening process, a shot can impinge more than once on the same place in a random manner; thus, it becomes difficult to predict the accumulated impingement effect in terms of final residual stress magnitude and distribution underneath the deformed surface by the Hertzian pressure theory. Therefore, experimental measurements by neutron diffraction and X-ray diffraction [9] methods are used to estimate compressive residual stresses produced by shot peening.

Most of the metal working processes (unless they are very carefully controlled) have a detrimental effect on fatigue life and resistance to stress corrosion cracking. Welding is the worst of them: welding creates very high residual tensile stresses and introduces a mechanical stress concentration area, a very hard brittle layer, and an annealed area, all in the heat affected zone (HAZ) adjacent to the weld metal. This combination can lower the fatigue strength to a small percentage of that of an integrally machined component (rather than welded). Peening can be applied to reduce the tensile stresses produced during the welding process improving the performance of the component. Figure 3 shows a T-butt specimen used in the experimental work during shot peening process and described in the following sections.

3. Fracture Mechanics Calculations

Fracture mechanics is a means to estimate whether or not a defect of given size will propagate under service loading and to calculate the degree of safety that the system owns against failure by fracture [21].

Fracture mechanics allows estimating the local conditions of stress and strain around a crack in terms of global parameters such as load, shape and size of the crack, geometry of the component, and material properties [22]. The most popular fracture mechanics parameter is the stress intensity factor (K); it can characterise the stress field ahead of a sharp crack according to the linear-elastic fracture mechanics theory.

4. Determination of Stress Intensity Factors

Various methods for the determination of K can be considered ranging from the consultation of handbooks to the application of complicated mathematical analysis with integral transforms and complex variables; numerical methods can also be considered such as the finite element method and the boundary element method and a final option can be the use of experimental techniques.

This paper provides results from the extraction of ΔK from experimental data; additionally, an analytical method is used to validate the experimental data. With the application of equipment able to provide crack growth measurements like the ACPD, the crack growth rate per cycle da/dN can be determined experimentally and knowing the fatigue constants of the material C and m, it is possible to apply Paris law [23] expressed in the following equation:

$$\frac{da}{dN} = C\,(\Delta K)^m$$
$$\Delta K = \left(\frac{1}{C}\frac{da}{dN}\right)^{1/m}. \quad (1)$$

Using crack growth data collected during experimental fatigue testing of a component, the calculated stress intensity factor would correspond to the specific conditions of loading, geometry of the component, and crack size variation during the test.

Life to failure can be determined rearranging the Paris equation proposed in the 1960s and still considered as the most widely accepted expression.

$$N_f = \int_{a_i}^{a_f} \frac{da}{C\,(\Delta K)^m}. \quad (2)$$

a_i has an important impact on life to failure estimation from (2) and direct measurement of a_i from welded specimens is imprecise as, for an edge crack, a_i can vary along the specimen width where initiation can take place. Thus, life to failure was determined directly from experiments when crack size penetrated through the full thickness.

Table 1: Data for experimentally tested T-butt specimens.

T-butt specimen	Repair profile (mm)	Shot peened	Specimen width (mm)	Thickness T (mm)	Notch SCF	Nominal stress (MPa)	LR (min/max)	Nominal stress range (MPa)
As welded	No	No	200	20	3.2	250	0.03	243
Edge repaired	$D = 4$; $R = 2$	No	200	30	3.4	82	0.1	74
Edge repaired & shot peened	$D = 4$; $R = 2$	Yes	200	30	3.4	112	0.1	101

The stress intensity factor range ΔK can also be expressed as

$$\Delta K = Y \Delta\sigma \sqrt{\pi a}. \tag{3}$$

Equation (3) is a general expression that can be applied to any crack geometry and loading mode by considering the corresponding Y factor. The Y factor varies as a function of various parameters.

For the calculation of the fatigue life of a crack repaired joint by crack removal, the Y factor should include the particular characteristics of the crack initiating in the repair notch and propagating through the thickness of the structural member.

Y factors can be obtained as the product of different effects and a recommended form is

$$Y = Y_s Y_w Y_e Y_g Y_k Y_m. \tag{4}$$

For the calculation of Y factors, various methods have been developed and can be broadly classified as empirical and analytical methods.

5. Extraction of Y Factors from Experimental Data

Empirical models are especially useful for the determination of Y factors for complex structural models due to the analytical difficulty in considering multiple factors that have an effect on crack growth and their interaction during crack growth evolution.

Crack growth experimental data presented here was obtained from T-butt fatigue repaired specimens. Crack growth rates, stress intensity factor range, crack shape characteristics, and Y factors were determined. In general, crack growth rates and ΔK are determined for the deepest point on the crack front for surface cracks and an average depth for edge cracks. Equations (5a), (5b), (6a), and (6b) were used to process the experimental data.

$$\frac{da_i}{dN_i} = C\left(\Delta K_i\right)^m \tag{5a}$$

$$\Delta K_i = \left[\frac{1}{C}\left(\frac{da_i}{dN_i}\right)\right]^{1/m}. \tag{5b}$$

Knowing values of ΔK_i and since $\Delta\sigma_i$ is known as it is defined for experimental purposes, a solution for Y_i factors can be obtained rearranging (6a) into (6b):

$$\Delta K_i = Y_i \Delta\sigma_i \sqrt{\pi a_i} \tag{6a}$$

$$Y_i = \frac{\Delta K_i}{\Delta\sigma_i \sqrt{\pi a_i}}. \tag{6b}$$

Y values are determined in this work for an as welded T-butt and fatigue crack repaired T-butt specimens to provide useful understanding of fatigue crack growth of repaired connections.

Parameters C and m in the Paris equation were set to $C = 4.5 \times 10^{-12}$ and $m = 3.3$ for da/dN in m/cycle and ΔK in MN m$^{-3/2}$. These values correspond to the upper bound obtained from a least squares geometric regression from experimental results obtained for BS 4360 50D steel in a laboratory air environment; minimum yield strength for thickness over 16 mm is 355 MPa [24].

6. Application of Compressive Residual Stresses for Fatigue Improvement

The application of compressive residual stresses to reduce the magnitude of tensile stresses on the repaired surfaces to improve the fatigue life of repaired connections was investigated. The shot peening technique was considered among needle peening and hammer peening due to its wide industrial application.

This paper aims to estimate Y factors produced by peening on a crack repaired component. The repair procedure is extensively described in [1, 16] and is based on the removal of the cracked material by grinding during early crack propagation stage. The repair profile is based on a selection of D, R, and repair length to design a specified geometry to reinstate a fatigue life that can be even larger than the as welded fatigue life.

7. Experimentally Determined Y Factors

Table 1 shows the shot peened and repair profile data for the experimentally tested T-butt specimens under pure bending loading. The geometry of the experimentally tested T-butt specimens, weld toe crack initiation location, and edge region where repair and peening are applied is shown in Figure 4.

Based on D and R dimensions selected for the crack removal, semicircular or U-shaped notches are produced. For

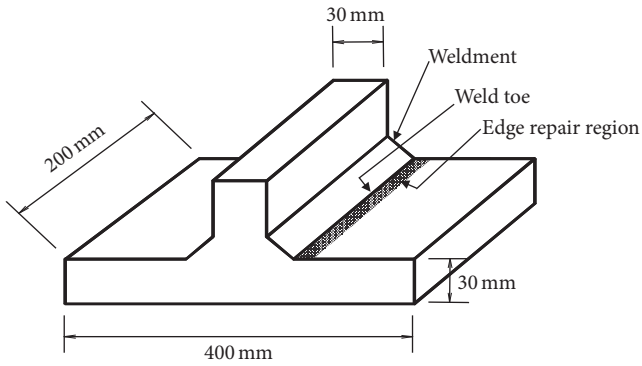

Figure 4: T-butt dimensions showing edge repair region and weld toe.

the $D \leq R$ case, a semicircular repair is produced and, for $D > R$, a U-shaped repair is produced. A graphical description of the U-shaped repair profile $D = 4$, $R = 2$ experimentally tested, based on Table 1 data, is shown in Figure 5.

A four-point bending set-up was used for fatigue testing, since it produces a constant moment distribution between the two internal loading points. The set-up consists basically of a top and bottom set of rollers which are bolted to a framework. The bottom set of rollers sits on a plate which has a hinge connection on top of the actuator. The hinge has the purpose of adjusting the set-up with the specimens. This adjustment is especially important in a four-point bending set-up to assure that each roller applies equal load to the specimen. The top set of rollers is fixed to the loading machine framework. The fatigue load is applied with a 1 Mega-Newton servohydraulic actuator controlled with a load or position controller (see Figure 6). Tests were performed under load control, so even when stiffness of the specimen changed as crack grows, the magnitude of the load cycle applied did not change.

Crack depth evolution was monitored from early stages of growth using the ACPD technique. The technique requires the injection of an alternating current on the surface of the specimen. The current follows the contour of surface breaking defects like cracks and since the potential gradient on the metal surface and on the crack faces is assumed to be linear, measurements of the potential difference across the crack and adjacent to the crack can be used for the calculation of the crack depth.

Experimental data for the T-butt fatigue tests is shown in Table 1; data details are as follows: tested specimens are coded as follows: as welded, edge repaired, and edge repaired and shoot peened. Repair profile dimensions define repair geometry type: U-shaped ($D > R$) or semicircular ($D \leq R$) (see Figure 5); the repair geometry used for the experiments was U-shaped $D = 4$ and $R = 2$. Edge repaired and shoot peened specimen has a repair profile with compressive residual stresses induced by shot peening. Specimen width is the total weld length along which at the weld toe edge repairs are machined, peening is applied, and edge cracks grow. Notch SCF is at the weld toe for the as welded specimen and in the bottom of the edge repairs where the crack initiates. Nominal stress is the stress unaffected by weldment, weld toe, and repair profile (see Figure 4). R is the ratio of min to max loads applied for testing. Nominal stress range is the difference between the max testing stress and min testing stress in a stress cycle unaffected by SCFs.

Cracks initiated along the specimen width at the weld toe for the as welded specimen and in the bottom of the repair profiles for the edge repaired specimens. Initial crack size a_i was not measured for fatigue life estimation purposes since the total fatigue life was experimentally determined when crack depth penetrated through the plate thickness. A fatigue life initiation to total fatigue life ratio of 0.2 was experimentally determined for the as welded specimen. Figure 7 shows a slice of a T-butt edge repaired specimen after fatigue testing; edge crack depth can be seen through the thickness but crack length along the edge repair is imperceptible for the naked eye. This is a relevant issue regarding fatigue crack inspection, since fatigue cracks cannot be detected on a routine surface visual inspection but crack depth can be almost through the full thickness.

Figure 8 shows fatigue crack growth versus number of load cycles for fatigue tested specimens. Crack growth rate and total fatigue life are different for the three specimens since they were designed with different features according to the objective of this research (see Table 1).

Figure 9 shows plots of da/dN versus crack depth and Figure 10 show plots of ΔK versus crack depth for the three tested specimens; it can be seen that the effect due to the differences between the specimens is consistent with Figure 8. A weight function flat plate curve is shown in Figures 9 and 10 which is explained further on when experimental results are validated.

Even though different nominal stress ranges were used for testing, experimental data allow estimating the compressive stress effect induced by peening on fatigue crack. Although Y factors do depend on load type, they do not depend on load level; thus Y factors were extracted and compared from experimental data, as explained when (6b) was introduced.

The hypothesis of the experiment was to consider the *"as welded T-butt"* specimen tested in an as welded condition as a reference for Y factors comparison. Thus, the Y factors obtained from the *"edge repaired T-butt"* are expected to be lower than the Y factors determined from *"as welded T-butt"* specimen, since the repair notch removed surface weld defects and the notch geometry was designed to have a similar SCF compared to the *"as welded T-butt"* specimen (see Table 1). Finally, Y factors from *"edge repaired + shot peened T-butt"* specimen are expected to be lower than Y factors determined from *"edge repaired T-butt"* specimen, since both specimens have the same notch repair geometry; thus SCFs are the same but induced compressive stresses by shot peening tend to inhibit crack initiation and crack propagation until a certain depth.

Experimentally determined Y factors are shown in Figure 11. The experimental Y values obtained from each one of the T-butt specimens in Table 1 provided information to validate the previously stated hypothesis as it is explained in the following section and also allowed the estimation of the compressive stress depth effect induced by shot peening.

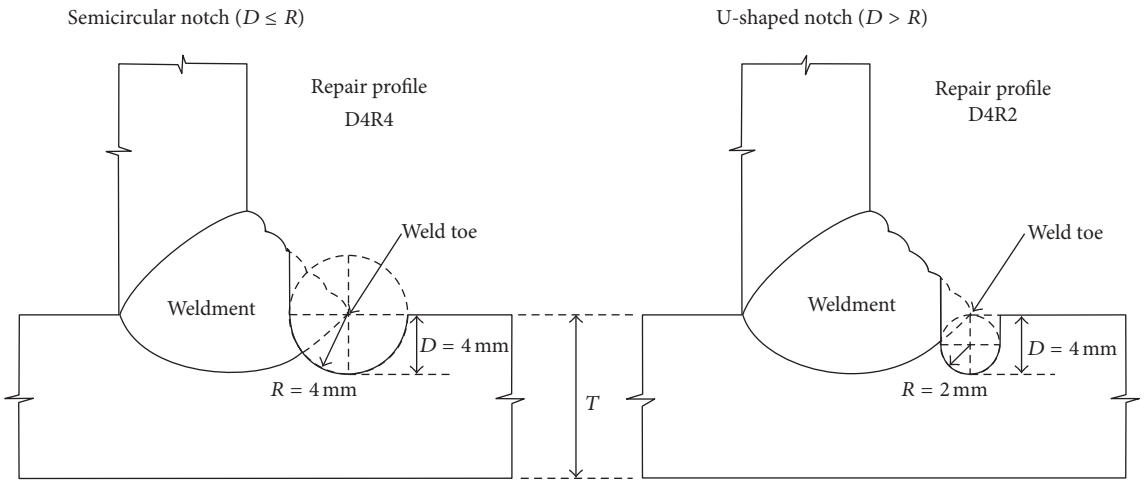

Figure 5: Semicircular and U-shaped repair profiles and dimensions.

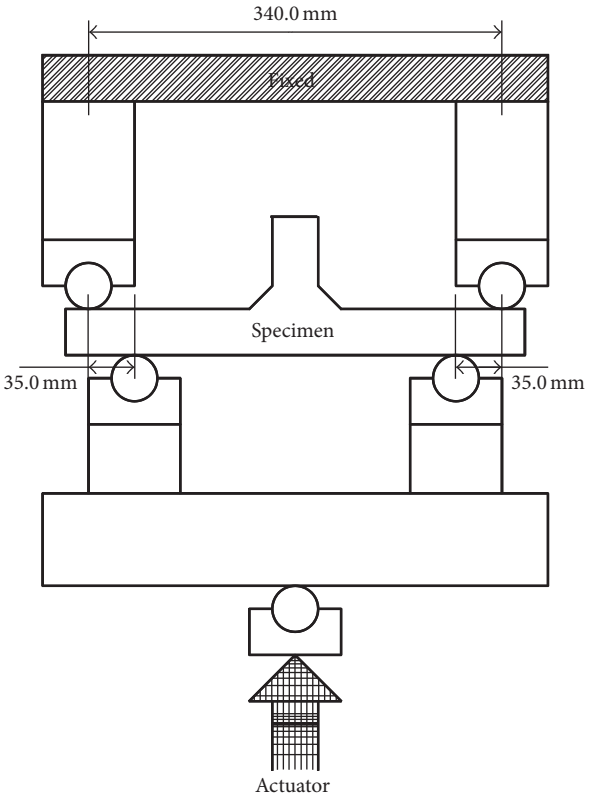

Figure 6: Loading set-up for fatigue testing.

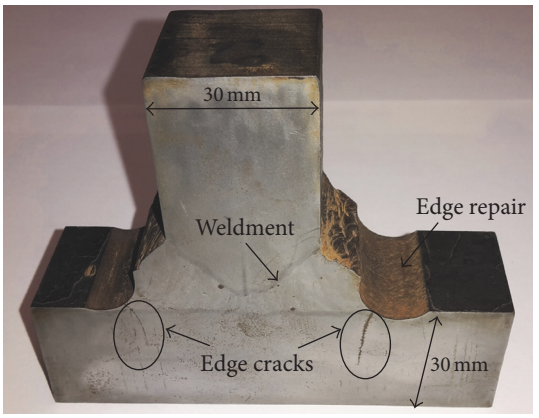

Figure 7: Slice of fatigue tested T-butt edge repaired specimen.

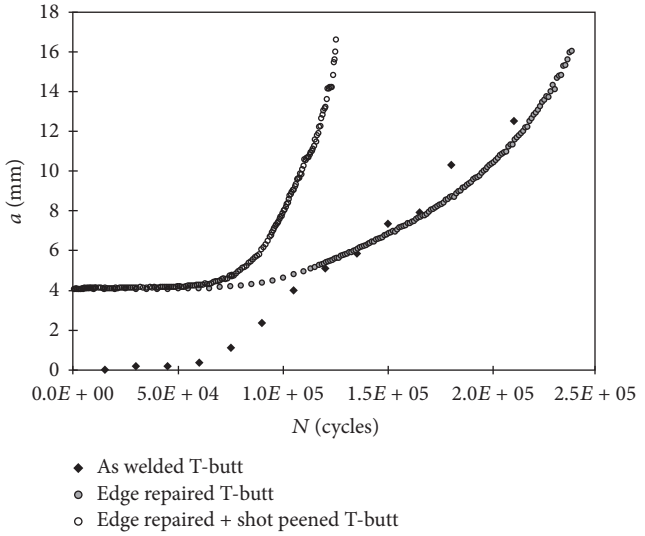

Figure 8: Fatigue crack growth versus number of load cycles for fatigue tested specimens.

From Figure 11, Y factors for the *"edge repaired + shot peened T-butt"* specimen are lower than the Y factors of *"edge repaired T-butt"* specimen. Since the only difference between these specimens is that the first one has a compressive stress layer induced by shot peening, it can be estimated that there is a crack initiation inhibition effect induced by the shot peening compressive stresses. However, once the crack initiates and propagates, there is a certain depth where the

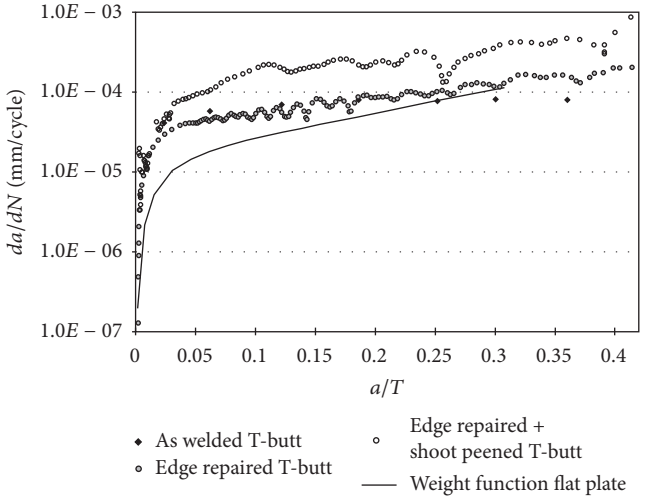

Figure 9: da/dN versus crack depth for fatigue tested specimens.

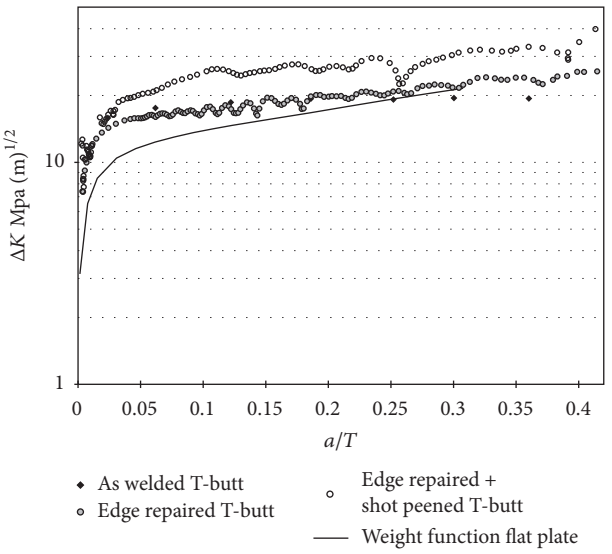

Figure 10: ΔK versus crack depth for fatigue tested specimens.

compressive stress layer effect is null; thus the Y factors for the *"edge repaired + shot peened T-butt"* specimen are similar to the ones of the *"edge repaired T-butt"* specimen. For this particular experiment, Y factors for the edge repaired specimens tend to be similar from $a/T > 0.07$. Since the only difference between these specimens is the compressive stress layer induced by shot peening, it can be estimated that the compressive stress layer depth is $a = 0.07T$. For the *"edge repaired + shot peened T-butt"* specimen, the plate thickness to consider is T minus 4 mm since crack initiation takes place at the bottom of the repair notch. Thus, the estimated compressive stress layer is $0.07(30 - 4) = 1.8$ mm for $T = 30$ mm.

Edge repaired specimens had a repair notch $D = 4$ mm and $R = 2$ mm at the weld toe along the total specimen width. These specimens were fatigue tested until failure and it was found that an edge crack developed at the bottom of the notch. The crack started almost simultaneously all along the

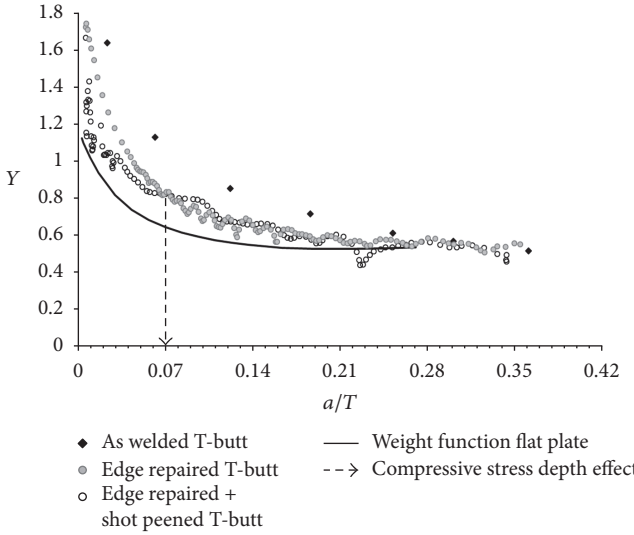

Figure 11: Experimental Y factors and estimation of residual compressive stress depth effect.

specimen width at the bottom of the notch, confirming the location of crack initiation and the area where shot peening has to be applied. This finding also confirms that it is not required to shot peen the walls of the repair notch, since cracking does not initiate there. This situation neglects the relevance of the impossibility that the striking material does not hit the walls of the notch at 90 degrees due to interference produced by the opposite wall when directing the nozzle to the target wall (see Figures 4 and 5).

8. Compressive Residual Stress Depth

Considering that the only difference between the *"edge repaired + shot peened T-butt"* and *"edge repaired T-butt"* specimens is the compressive stress layer induced by shot peening, the compressive stress layer depth has been estimated from Figure 12 as the depth from which Y factors are similar. From the experimental results, the compressive stress layer has been estimated in the order of 1.8 mm for BS 4360 50D used for the T-butt.

From a literature review, compressive residual stress distribution is reported by Hoffmeister et al. [16] for a residual stress relaxation study in shot peened samples made of Ni-based superalloy IN718 and by Tosha [17] for a study on the effect of shot peening on surface integrity and residual stress distributions induced by shot peening for a medium carbon steel (S45C) and a carburized steel (SCM415). Residual stresses were measured by X-ray diffraction stress analyses. Although the objective of the first study is to determine the relaxation effect varying the temperature and time for stress relieve, Figure 12 provides the residual stress distribution at room temperature (RT) before residual stress is relieved; the maximum shot peening residual stress is at depth $X_{\max} = 70\,\mu$m and the depth where residual stress is nil is at $X_0 = 220\,\mu$m. For the second study, Figure 13 shows shot peening residual stress distributions varying shot diameter (D) and

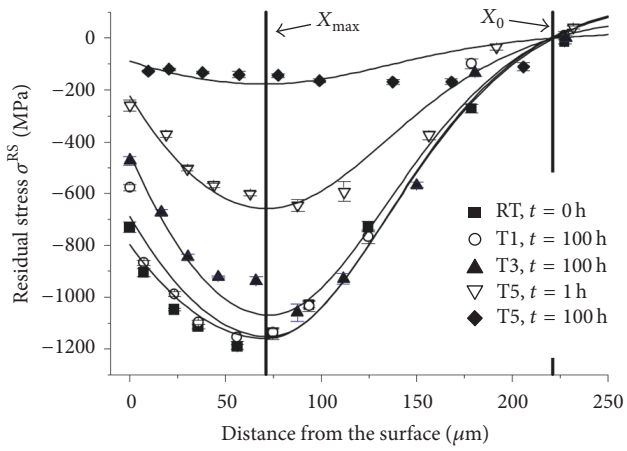

Figure 12: Shot peening residual stress depth distributions for various heat relaxation treatments (RT: room temperature; X_{max} = 70 μm and X_0 = 220 μm) [16].

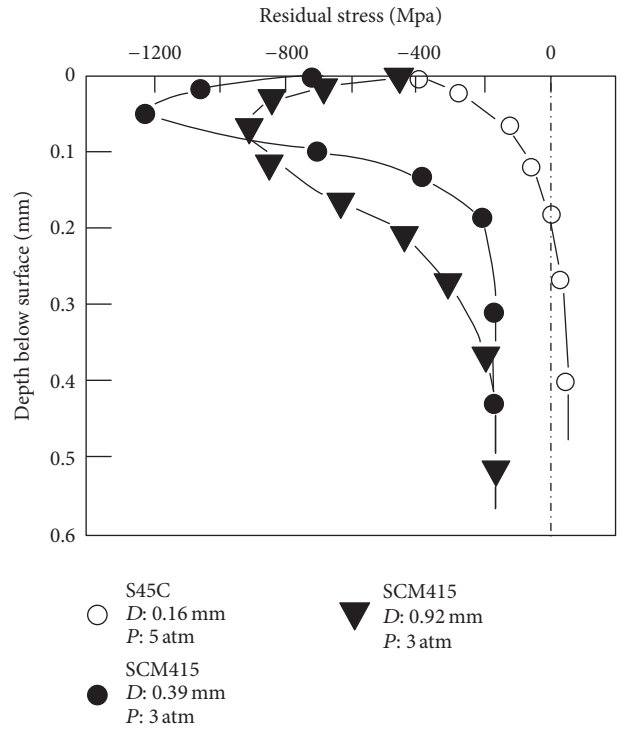

Figure 13: Residual stress distributions induced by shot peening for a medium carbon steel (S45C) and a carburized steel (SCM415) [17].

blast pressure (P); it can be seen that for the medium carbon steel (S45C) the residual stress is nil at approximately 0.2 mm depth. For the carburized steel (SCM415) the stress distribution plot does not show the depth where the residual stress is nil; it can be deduced that it is definitively deeper than 0.6 mm.

Direct comparison of experimentally determined shot peening compressive stress layer of 1.8 mm with shot peening compressive stress layers reported by Hoffmeister et al. [16] and by Tosha [17] is not feasible, since shot peening data

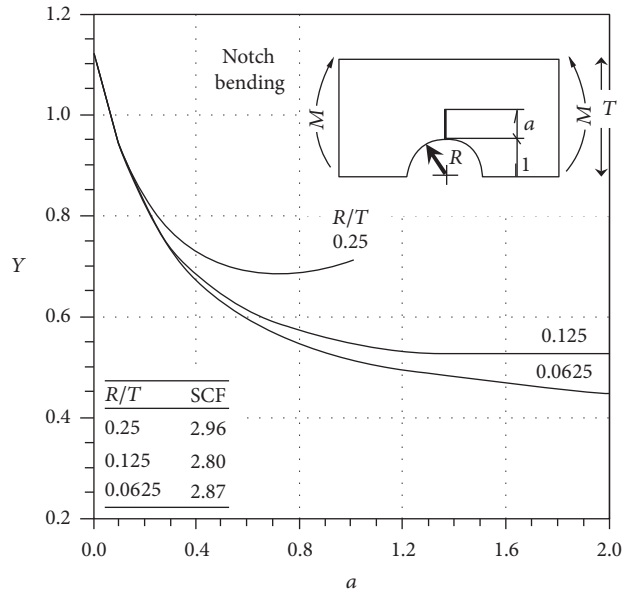

Figure 14: Weight function Y factors for an edge crack at a semicircular notch in an infinite plate subjected to in plane bending [18].

like time of exposure, shot size, and blast pressure which determine the residual stress depth distribution cannot be correlated.

Thus, validation of experimental results would be done by comparison against weight function Y factors.

9. Weight Function versus Experimental Y Factors

In order to validate the experimental results, analytical Y factors were determined by using the weight function developed by Wu and Carlsson [18] presented in Figure 14 for a similar edge repair profile used in the experimentally tested specimens under bending load. From Figure 14, it is possible to identify that Y factors do not depend on load level but do depend on load type which is bending for the case studied.

The weight function corresponds to an edge crack at a semicircular notch in an infinite plate. From Figure 14, weight function Y factors consider R centre on the surface of the plate; thus, given D = 4 mm, the R value has to be 4 mm (see Figure 5). On the other hand, the repair profile used for the experiments is D = 4 mm and R = 2 mm, which is a U-shaped repair notch with R centre 2 mm below the surface of the plate (see Figure 5). Thus, Y factors by the weight function were determined for D = 4 mm and R = 4 mm notch geometry and compared with the experimentally determined Y factors for D = 4 mm and R = 2 mm repair notch as shown in Figure 11.

There are two main differences between the weight function model shown in Figure 14 and the experimentally tested T-butt specimens: (1) *weldment effect:* available weight function Y factors data is for edge repaired flat plates and experimental Y factors data correspond to repaired T-butts; (2) *notch geometry:* weight function Y factors data is for a

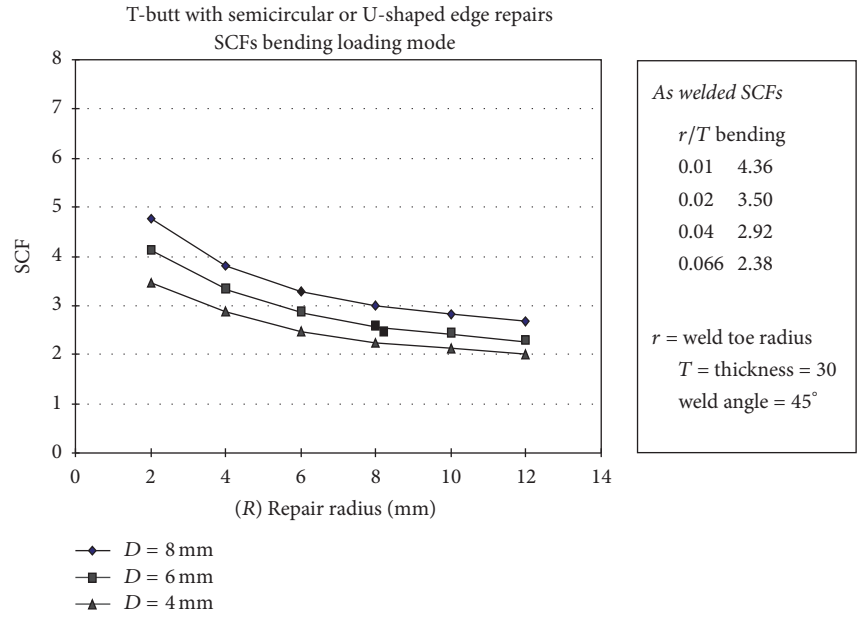

Figure 15: Stress concentration factors for a T-butt with semicircular and U-shaped edge repairs under bending loading [19].

semicircular notch and experimental data correspond to a U-shaped notch edge repair.

It is expected that the weight function Y factors values are lower than the experimental T-butt Y factors values shown in Figure 11, since the weight function Y factors correspond to an infinite flat plate; thus, they do not have the stress concentration effect produced by the T-butt weldment.

Despite the two main differences mentioned, the weight function Y factors data allow validating the experimental results, since both data sets follow a similar distribution as shown in Figure 11 and an explanation of magnitude differences has been identified and described as follows:

(1) *Weldment effect: edge repaired flat plates versus T-butts Y factors.* The experimental Y factors were determined from crack data recorded in the bottom of U-shaped edge repairs. The U-shaped edge repairs removed the weld toe; thus, the weld toe effect is erased and the only weld effect that remains is due to the weldment geometry (see Figure 5).

Analytical findings on notch repair geometry reported by Rodriguez et al. [19] confirmed that the weld toe effect is erased in a weld notch repair and the weldment geometry effect is reduced as the repair radius increases.

From Figure 15, the fatigued specimens with repair geometry $D = 4$ mm and $R = 2$ mm have an SCF = 3.4 which is higher than SCF = 2.9 that corresponds to the average SCF value of a flat plate weight function solution $D = 4$ mm and $R = 4$ mm (see Figure 14). Thus, experimental Y factors are expected to be moderately higher than estimated by the weight function until the weldment effect is nil as crack depth propagates through the thickness, as can be seen in Figure 11 for $a/T > 0.20$.

(2) *Notch geometry: semicircular weight function versus U-shaped experimental Y factors.* The concept of equivalent notch configurations establishes that, for any given notch geometry, there is always an equivalent U notch with the same maximum stress at the notch root [20] (see Figure 16). Thus, SCF values from U-shaped and semicircular notches are equivalent, given that D and R values are the same for both cases.

The repair geometry difference between the experimental work and the weight function is due to increasing R from 2 to 4 mm, respectively (see Figure 5). From Figure 15, it can be observed that, for $D = 4$ mm as used in the experiments and in the weight function, a change in R from 2 mm to 4 mm provides a SCF reduction from 3.4 to 2.9 which is a 15% stress difference. Therefore, it is expected that the weight function Y factors are moderately lower than obtained experimentally within the range where weldment and notch geometry have an influence $0 < a/T < 0.20$ (see Figure 11). As crack propagates through the thickness, the weldment and notch geometry effect on Y factors fade out and beyond $a/T > 0.17$ weldment and notch geometry have no influence on crack propagation; thus experimental and weight function Y factors are the same.

10. Discussion

A T-butt welded edge repaired weight function solution is not available in the published literature; the most similar available solution corresponds to an edge repaired flat plate. The absence of weldment geometry leads to an approximate SCF reduction of 18% at the notch compared to the T-butt case (flat plate from Figure 14, D4R4, $T = 30$, SCF = 2.8; and T-butt from Figure 15, D4R2, $T = 30$, SCF = 3.4); thus, flat plate Y factors are lower in early stages of crack growth. Once

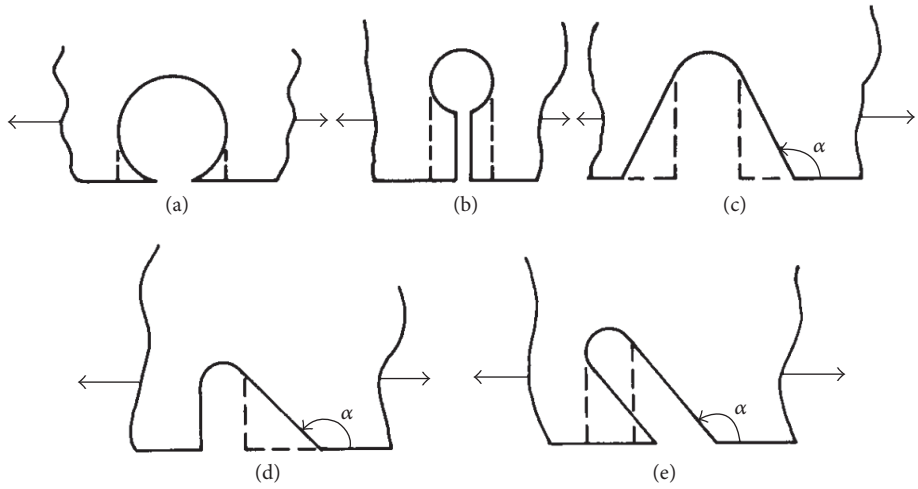

Figure 16: Equivalent notch configurations [20].

the crack propagates, the weldment SCF influence decreases and Y factors for the flat plate weight function and T-butt experimental data tend to merge for $a/T > 0.20$ as shown in Figure 11.

Although weight function data versus T-butt experimentally determined Y factors have two main differences, weldment effect and notch geometry, the experimental results showed that the weldment and notch geometry effects become nil as crack propagates through the thickness $a/T > 0.20$ (see Figure 11), thus validating the experimentally determined Y factors.

Based on validated Y factors experimental data, difference between *"edge repaired + shot peened T-butt"* and *"edge repaired T-butt"* specimens is the compressive stress distribution layer induced by shot peening and included in Y factors as Y_g. However, it is not possible to estimate Y_g isolated effect. From Figure 11, it is possible to estimate a layer of 1.8 mm depth where the residual compression stress induced by peening has a retardant influence on crack growth in fatigue crack repaired weldments. This finding cannot be extrapolated due to the reduced sample of repaired T-butt specimens tested. For a future research, it is recommended to extend the scope of the experimental work to investigate the effect of parameters such as time of exposure, blast pressure, and shot size in the residual compressive stress induced by shot peening.

A relevant observation regarding life extension of fatigue cracked welds by notch repair can be derived from the analysis of experimental SCF data reported in this work. The repair geometry $D = 4$ mm and $R = 2$ mm has an approximate SCF = 3.4 (see Figure 15), and this value is close to an average value of an as welded T-butt SCF = 3.2 (see right-hand side box in Figure 15). This means that, by appropriately designing a repair geometry, the repaired profile SCF can be similar to the as welded condition. A comparison of the as welded and repaired profiles SCFs in Figure 15 shows the possibility to identify repair notch dimensions with even lower SCF values than in as welded condition. For example, the repair geometry $D = 4$ mm and $R = 2$ mm has a SCF = 3.4 which is lower than a SCF = 4.36 that corresponds to $r/T = 0.01$ as welded T-butt.

11. Conclusions

Stress intensity factors for a set of as welded, edge repaired peened, and edge repaired unpeened T-butt specimens were experimentally determined. The as welded T-butt specimen provided the base line of stress intensity factors to compare with. Stress intensity factors from peened and unpeened edge repaired T-butt specimens allowed depth estimation of compressive residual stresses induced by peening in a fatigue crack repair notch. A residual compressive stress layer of 0.07 of the plate thickness was estimated for the fatigue tested specimens. This finding cannot be extrapolated, since the residual stress compressive layer induced by peening depends on time of exposure, blast pressure, and shot size; thus, these three parameters can vary for each peening application. Experimental estimation of the peening effect on stress intensity factors in fatigue crack repaired weldments was validated by comparison against the analytical weight function solution for an edge repaired flat plate. From experimental comparison of stress intensity factors, a preliminary estimate is that peening has a limited effect on crack propagation inhibition for fatigue crack repaired T-butt specimens subjected to bending loading.

Nomenclature

a: Crack depth
a_i: Initial crack length
a_f: Final crack length
ACPD: Alternating Current Power Drop
C: Material constant
d: Pellet diameter
D: Repair depth
da/dN: Crack growth rate
HAZ: Heat affected zone
m: Material constant

N_f: Cycles to failure
Y: Modification factor (Y factor)
Y_i: Y factor "i"
Y_s: Correction for a free front surface
Y_w: Correction for finite plate width
Y_e: Correction for crack geometry
Y_g: Correction for nonuniform stress field
Y_k: Correction for the presence of geometrical discontinuity
Y_m: Correction for changes in structural restraint
K: Stress intensity factor
K_{res}: Residual stress intensity factor due to welding process
ΔK: Stress intensity range $K_{\max}-K_{\min}$
ΔK_i: Stress intensity range "i"
N_i: Number of cycles at ΔK_i and a_i
r: Weld toe radius
R: Repair radius
LR: Minimum load/maximum load
SCF: Stress concentration factor
T: Plate thickness
W: Plate width
$\Delta\sigma$: Surface stress range of uncracked welded joint at the crack site
$\Delta\sigma_i$: Surface stress range "i" of uncracked welded joint at the crack site
α: Repair orientation.

Conflicts of Interest

The authors declare that there are no conflicts of interest regarding the publication of this paper.

References

[1] J. E. Rodriguez-Sanchez, W. D. Dover, and F. P. Brennan, "Application of short repairs for fatigue life extension," *International Journal of Fatigue*, vol. 26, no. 4, pp. 413–420, 2004.

[2] P. J. Haagensen and S. J. Maddox, *TIG Dressing and Hammer Peening for Steel and Aluminium Structures, IIW Recommendations for Weld Toe Improvement by Burr Grinding*, 1998.

[3] P. J. Haagensen, "Repair and Strengthening of the Veslefrikk B Floating Production Platform," pp. 2000–2394, OMAE Paper, New Orleans, LA, USA, 2000.

[4] J. E. Rodríguez-Sánchez, A. Rodríguez-Castellanos, F. Pérez-Guerrero, M. F. Carbajal-Romero, and S. Liu, "Offshore fatigue crack repair by grinding and wet welding," *Fatigue and Fracture of Engineering Materials and Structures*, vol. 34, no. 7, pp. 487–497, 2011.

[5] A. Hobbacher, *Recommendations for Fatigue Design of Welded Joints and Components*, IIW document IIW-1823-07ex XIII-2151r4-07/XV-1254r4-07, International Institute of Welding, 2008.

[6] British Standards Institution, "Guidance on methods for assessing the acceptability of flaws in fusion welded structures," Document, BSI Published, 1991.

[7] *Assessment of the Integrity of Structures Containing Defects, R6, Revision 4*, British Energy Generation Ltd, Barnwood, 2001.

[8] J. Y. Barthelemy, *Structural Integrity Assessment Procedures for European Industry—SINTAP. Compendium of residual stress profile*, SINTAP, Institut de Soudure, 1999.

[9] H.-Y. Lee, F. R. Biglari, R. Wimpory, and K. M. Nikbin, "Treatment of residual stress in failure assessment procedure," *Engineering Fracture Mechanics*, vol. 73, no. 13, pp. 1755–1771, 2006.

[10] A. M. Al-Mukhtar, "Residual stresses and stress intensity factor calculations in T-welded joints," *Journal of Failure Analysis and Prevention*, vol. 13, no. 5, pp. 619–623, 2013.

[11] R. Bao, X. Zhang, and N. A. Yahaya, "Evaluating stress intensity factors due to weld residual stresses by the weight function and finite element methods," *Engineering Fracture Mechanics*, vol. 77, no. 13, pp. 2550–2566, 2010.

[12] J. Liu, "Numerical analysis for effects of shot peening on fatigue crack growth," *International Journal of Fatigue*, vol. 50, pp. 101–108, 2013.

[13] J. Liu, H. Yuan, and R. Liao, "Prediction of fatigue crack growth and residual stress relaxations in shot-peened material," *Materials Science and Engineering A*, vol. 527, no. 21-22, pp. 5962–5968, 2010.

[14] K. J. Marsh, *Shoot Peening: Techniques and Applications*, Engineering Materials Advisory Services Ltd, 1993.

[15] A. Bignonnet, H. P. Lieurade, and L. Picouet, *Improvement on the Fatigue Life of Offshore Welded Connections*, Institut de Recherches de la Siderurgie Francaise (IRSID).

[16] J. Hoffmeister, V. Schulze, A. Wanner, R. Hessert, and G. Koenig, "Thermal Relaxation of Residual Stresses induced by Shot Peening," in *Procceding of the 10th International Conference on Shot Peening (ICSP-10 '08)*, Tokyo, Japan, 2008, Doc No.2008060.

[17] K. Tosha, "Effect of shot peening on surface integrity," in *Procceding of the 10th International Conference on Shot Peening (ICSP-10 '08)*, Tokyo, Japan, 2008, Doc No.2008056.

[18] X. R. Wu and A. J. Carlsson, *Weight Functions and Stress Intensity Factor Solutions*, Pergamon Press, 1991.

[19] J. E. Rodriguez, F. P. Brennan, and W. D. Dover, "Minimization of stress concentration factors in fatigue crack repairs," *International Journal of Fatigue*, vol. 20, no. 10, pp. 719–725, 1998.

[20] O. L. Bowie and C. E. Freese, "Analysis of Notches Using Conformal Mapping Stress analysis of notch problems," in *Mechanics of Fracture*, G. C. Sih, Ed., vol. 5, Noordhoff Int. Publishing, 1978.

[21] G. Wanlin and P. Withey, *Fracture Mechanics Worked Examples*, The Institute of Materials, 1993.

[22] A. Almar-Naess, *Fatigue Handbook*, Tapir, 1985.

[23] P. C. Paris and F. Erdogan, "A critical analysis of crack propagation laws," *Journal of Basic Engineering*, vol. 85, 1963.

[24] UKORSP, Final Report to the European Coal and Steel Community, 1979.